Journal of the European Ceramic Society 21 (2001) 1597–1600

www.elsevier.com/locate/jeurceramsoc

Morphology and electrical properties of $SrTiO_3$-films on conductive oxide films

K. Reichmann [a,*], T. Schneller [b], S. Hoffmann-Eifert [c], U. Hasenkox [b], R. Waser [b]

[a] *Institut für Chemische Technologie anorganischer Stoffe, TU-Graz, Stremayrgasse 16/III, A-8010 Graz, Austria*
[b] *Institut für Werkstoffe der Elektrotechnik, RWTH-Aachen, Sommerfeldstraße 24, D-52074 Aachen, Germany*
[c] *Institut für Festkörperforschung, Forschungszentrum Jülich, D-52425 Jülich, Germany*

Received 4 September 2000; received in revised form 23 October 2000; accepted 25 October 2000

Abstract

The effect of various electrically conductive oxides on the morphology and the electrical properties of $SrTiO_3$ films (STO) was investigated by means of scanning electron microscopy, impedance analysis and leakage current measurement (DC). $LaNiO_3$ (LNO), $La_{0.5}Sr_{0.5}CoO_3$ (LSCO) and $La_{0.7}Sr_{0.3}MnO_3$ (LSMO) as electrically conductive oxides were deposited on platinized silicon wafers by chemical solution deposition (CSD) via the propionate route. Subsequently a film of STO was deposited by CSD of an acetate based precursor solution. Platinum contacts were sputtered onto the STO film to act as top electrodes. The STO films in these multilayer structures showed significant differences to STO films grown directly on the platinized substrate with respect to morphology as well as to the electrical properties.

Keywords: Capacitors; Chemical solution deposition; Electrical properties; Electron microscopy; Perovskites

1. Introduction

Electrically conductive oxides with perovskite structure are interesting candidates for electrodes in thin film multilayer structures with other perovskite type materials. Recently, such electrodes have been tested in FERAM cell structures with $Pb(Zr,Ti)O_3$ (PZT) for the reduction of the fatigue problem.[1,2] The aim of this work was to study the electrical characteristics of $SrTiO_3$ films (STO) with different electrode materials in a capacitor design. All films were deposited by chemical solution deposition (CSD), which is a versatile method providing excellent control over film stoichiometry.[3]

As electrically conductive oxides we tested $LaNiO_3$, $La_{0.5}Sr_{0.5}CoO_3$ and $La_{0.7}Sr_{0.3}MnO_3$ (in the following written as LNO, LSCO and LSMO, respectively). LNO is reported to be a Pauli-paramagnetic, *n*-type metallic conductor.[4,5] The conductivity of LNO is found to be around 10^3 S/cm at room temperature. LSCO is a *p*-type conductor with a conductivity of about 10^4 S/cm at room temperature,[6] which is strongly influenced by the oxygen deficiency of the perovskite. The conductivity of the thin films is found to be some orders of magnitude lower. The conductivity (also *p*-type) of LSMO is found to be around 10 S/cm at room temperature.[7,8] Additionally, a pronounced temperature dependence has to be taken into account due to the colossal magneto-resistance (CMR) effect.[9]

STO is a classical model material for perovskite type alkaline earth titanates. The phase is cubic above 105 K,[10] thus the material is paraelectric in the temperature range under investigation. The electrical properties and the charge transport mechanisms are not influenced by spontaneous polarization.[11–13]

2. Experimental

For the preparation of the solutions for the deposition of the conductive oxides the propionate route, described by Hasenkox[14,15] was chosen. In the case of STO the acetate route according to Hoffmann[16,17] was selected.

The propionate solutions for the conductive oxides were synthesized from commercially available acetates $[La(OOCCH_3)_3{\cdot}3H_2O$ (Merck), $Sr(OOCCH_3)_2$ (Merck),

* Corresponding author. Tel.: +43-316-873-8294; fax: +43-316-873-8272.
E-mail address: k.reichmann@tugraz.at (K. Reichmann).

0955-2219/01/$ - see front matter
PII: S0955-2219(01)00073-5

$Mn(OOCCH_3)_2{\cdot}4H_2O$ (Aldrich), $Co(OOCCH_3)_2{\cdot}4H_2O$ (Merck), $Ni(OOCCH_3)_2{\cdot}4H_2O$ (Lancaster)] by dissolving the appropriate stoichiometric amounts of each compound in propionic acid and distilling off the liberated acetic acid. To remove water of crystallization a slight stoichiometric excess (approximately 5%) of propionic acid anhydride was added to the reaction mixture. After removal of the acetic acid and a great portion of the propionic acid the solution was diluted with butanol and propionic acid to give a 0.1 molar solution in propionic acid/butanol ratio of 2:1. These precursor solutions are moisture insensitive and can be handled in ambient atmosphere. For the STO precursor tetrabutyltitanium (TBT from Merck) was stabilized with acetylacetone (twice the molar amount of TBT) and Sr-acetate was added. This mixture was diluted with 2-methoxyethanol and acetic acid to give a 0.1 molar solution in acetic acid/2-methoxyethanol 2:1. Due to the stabilizing effect of acetylacetone (and also 2-methoxyethanol) for the titanium compound this solution was stable in ambient atmosphere at least for one month.

The conductive oxides were deposited on 1×1 inch pieces of oxidized silicon wafers from aixACCT as substrates (Si/SiO_2) for the measurement of the conductivity parallel to the film plane. STO was deposited on 1×1 inch pieces of platinized silicon wafers ($Si/SiO_2/TiO_2/Pt$) from Radiant and impedance was measured perpendicular to the film plane with dots of platinum (1 mm^2) sputtered on top of the dielectric layer to serve as top electrode. The substrates were cleaned by conventional methods (acetone-, isopropanol- and water-bath in ultrasound). The pieces of platinized wafers were heated at 700°C/30 min in oxygen before coating.

The deposition of the conductive oxides was done by spin-coating at 500 rpm for 5 s followed by 4000 rpm for 30 s with a subsequent pyrolysis step on a hot plate at 350°C for 2 min in air. This sequence was repeated 10 times with a final crystallization step at 750°C for 15 min in oxygen in a quartz tube furnace to yield a film of about 90 nm thickness (checked with a DEKTAK profilometer). In the case of STO the film was crystallized after each spin-coating at 750°C for 15 min in oxygen. After 20 deposition/crystallization cycles the whole layer was heated at 800°C for 30 min in oxygen. The total thickness of the STO layer was about 180 nm.

For the multilayer structures the conductive oxides were deposited on the platinized wafers and served as bottom-electrode for the dielectric layer. Subsequently the STO was deposited in the way described above. Afterwards dots of platinum (1 mm^2) were sputtered on top of the dielectric layer to serve as top electrode. The characterization of the single layers and the multilayer structures was done by X-ray diffraction (Philips 1730), scanning electron microscopy (LEO Gemini DSM 982) and AC/DC-methods (Solartron 1260 Impedance Analyzer, Keithley 6517 Electrometer).

3. Results and discussion

The single layers of LNO, LSCO and LSMO proved to be polycrystalline, even and smooth films. The morphology of the conductive oxide films exhibits some difference with respect to the granularity of the structure. LSMO has the smallest grain size and the films are very dense whereas the LNO and LSCO films consist of larger grains with pores in between. The STO films consist of columnar grains, which is due to the crystallization after each coating step. The formation of the perovskite phase was confirmed by XRD in all cases. The conductivity of the conductive oxides measured on strip-like test structures is listed in Table 1. It can be seen that the conductivity is the highest for the LNO film.

Fig. 1 shows the multilayer structures of the conductive oxides on platinized wafers serving as bottom electrodes for the STO layer on top in comparison to the STO film directly grown on the platinized wafer. It can be seen that the columnar structure of the STO is maintained in principle in all cases of conductive oxides as bottom electrode. Compared to the morphology of the STO film on Pt [Fig. 1(a)] the diameter of the STO columns grown on LNO [Fig. 1(b)] is obviously reduced. On LSCO [Fig. 1(c)] and LSMO [Fig. 1(d)] the STO film seems to exhibit a denser microstructure and grain boundaries appear to be more blurred.

Fig. 2 shows the spectra of impedance and capacitance measured perpendicular to the film plane (with Pt dots on the STO as top electrodes). Up to 100 kHz commonly the impedance is about 100 kΩ and the capacitance about 10 nF. The resonance that appears between 100 kHz and 1 MHz in the capacitance curve is due to the experimental set-up and does not show a specimen property. Generally, the impedance properties of the specimens with conductive oxide electrodes show characteristics similar to the specimen with symmetric platinum electrodes. The sample with LSMO as bottom electrode exhibits only weak frequency dependence up to 10 kHz for impedance and capacitance. Also, for samples with LNO as bottom electrode, the capacitance remains almost constant in the lower frequency range, but the absolute value of the capacitance is the lowest of all samples. On the other hand the specimen with LSCO electrodes exhibits a pronounced increase of the capacitance in the low frequency range. With ceramic capacitors such an effect is observed in the case of a porous dielectric layer.

Table 1
Conductivity of conductive oxide films

Material	Thickness of film (nm)	Conductivity (S/cm)
LNO	85	480
LSMO	95	8.9
LSCO	85	8.7

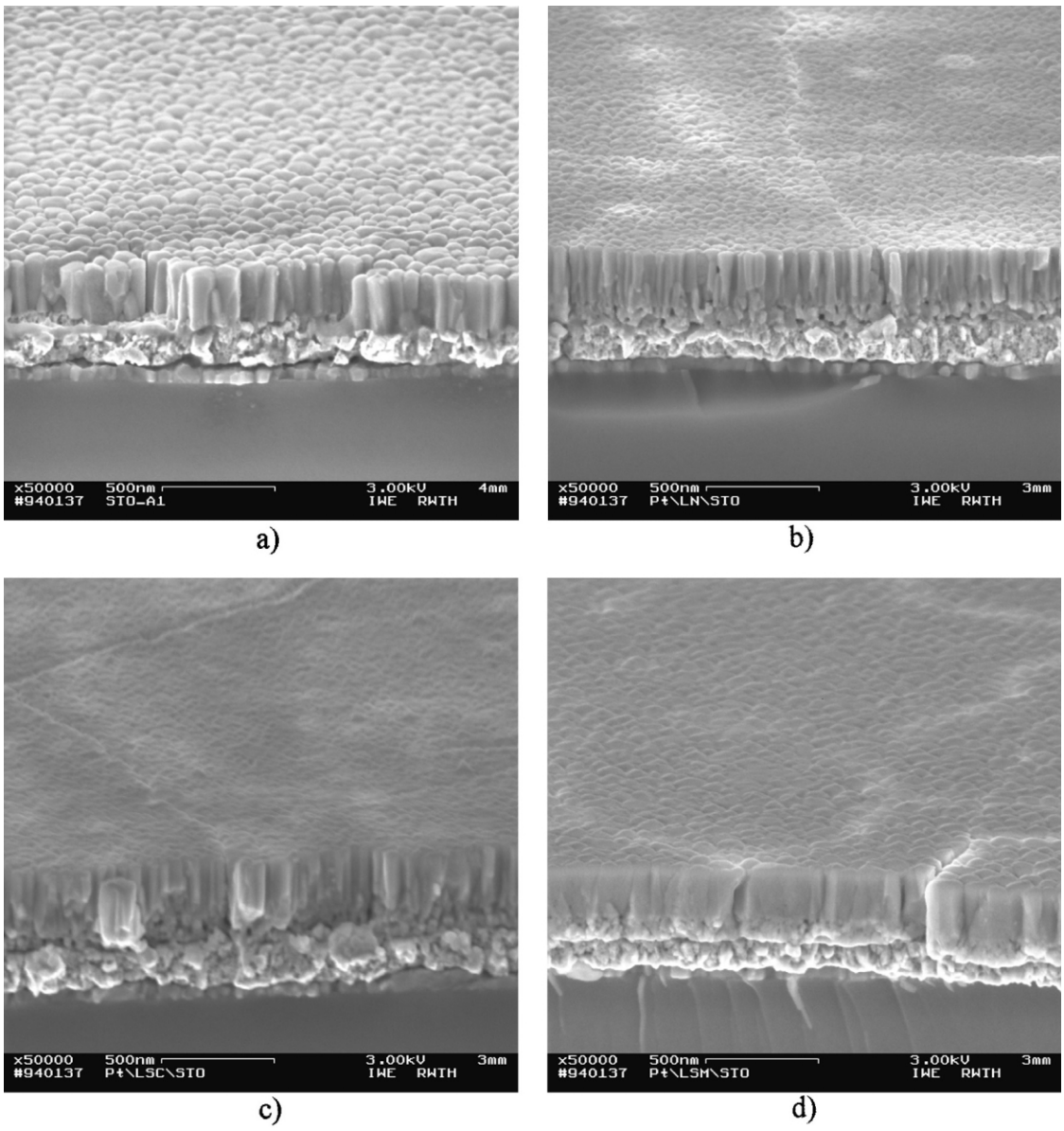

Fig. 1. STO film grown directly on the platinized Si wafer (a) and with LNO (b), LSCO (c) and LSMO (d) films in between. Edge view of the broken sample.

Leakage currents (DC) were measured as a function of the applied voltage. From Dietz[13,18] it is known that the cathode material has a major impact on the leakage current density. Therefore, attention was paid to making the bottom electrode at cathode potential. Fig. 3 shows the leakage current density vs. electric field (with field equal to voltage divided by the thickness of the STO film) at room temperature. The highest field corresponds to a voltage of 10 V on the specimen. The specimen with symmetrical platinum electrodes exhibit low current densities in the so called ohmic region (low field) and a transition into a varistor characteristics close to 10^7 V/m. These results are comparable to that of Dietz[13,18] and Hoffmann.[17] Similar values of leakage current densities are found in specimens with LNO-electrode. The transition to the varistor region again is found at 10^7 V/

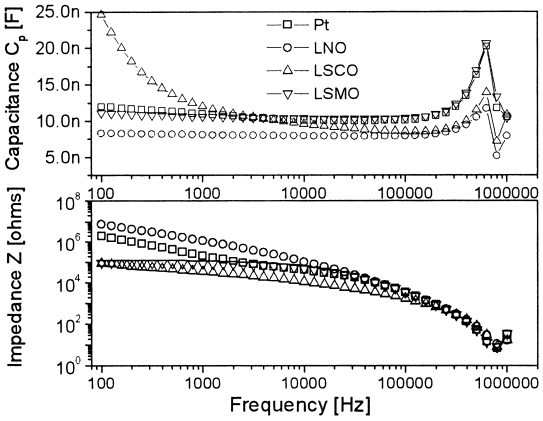

Fig. 2. Spectra of impedance and capacitance of the STO film on Pt and conductive oxide electrodes measured perpendicular to the film plane.

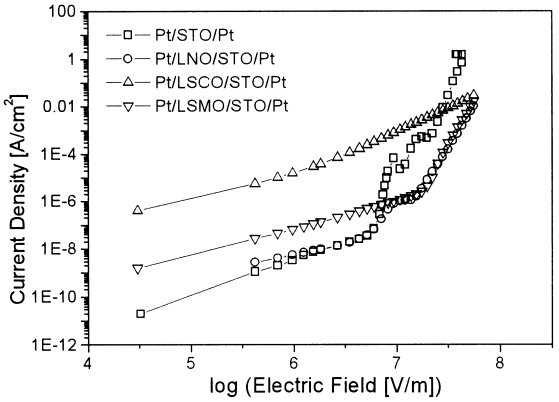

Fig. 3. Leakage current density vs. electric field at room temperature of the STO film on Pt and conductive oxide electrodes.

m, but the curve then follows the characteristics of the specimen with LSMO electrode. The leakage current density of the specimen with LSMO electrode is found to be one to two orders of magnitude higher than that of the specimen with Pt electrodes, but the transition to the varistor region is also significantly higher. The specimen with LSCO electrode shows the highest leakage current densities but no transition to the varistor region could be observed up to 10^8 V/m (20 V on the specimen).

4. Conclusions

CSD of alkoxides has proven to be a viable method for the preparation of multilayer structures of conductive oxides and STO. The STO films grown on conductive oxides (LNO, LSCO and LSMO) exhibit some differences with respect to morphology compared to films grown directly on the platinized substrate. Nevertheless, impedance spectra indicate that in principle specimens with oxide bottom electrodes work as capacitors with similar characteristics as specimens with Pt as bottom electrode. Significant differences are revealed by the leakage current measurements. STO films on LNO and Pt exhibit the same characteristics of the leakage current vs. electric field. With LSMO and LSCO higher leakage currents are found, but additionally the varistor region is pushed towards higher fields.

Acknowledgements

K.R. was supported by the Austrian Science Foundation with an Erwin-Schroedinger-Scholarship under the contract No. J1697-CHE.

References

1. Ramesh, R., Gilchrist, H., Sands, T., Keramidas, V. G., Haakenaasen, R. and Fork, D. K., Ferroelectric La–Sr–Co–O/Pb–Zr–Ti–O/ La–Sr–Co–O–heterostructures on silicon via template growth. *Appl. Phys. Lett*., 1993, **63**(26), 3592–3594.
2. Aggarwal, S., Song, T. K., Dhote, A. M., Prakash, A. S., Ramesh, R., Velasquez, N., Boyer, L. and Evans, J. T. Jr., Influence of cationic stoichiometry of $La_{1-x}Sr_xCoO_3$ electrodes on the ferroelectric properties of lead based thin film memory elements. *J. Appl. Phys*., 1998, **83**(3), 1617–1624.
3. Waser, R., *Current Opinion in Solid State and Materials Science*, 1996, **1**, 706–714.
4. Rajeev, K. P., Shivashankar, G. V. and Raychaudhuri, A. K., Low-temperature electronic properties of a normal conducting perovskite oxide ($LaNiO_3$). *Solid State Commun*., 1991, **79**(7), 591.
5. Sreedhar, K., Honig, J. M., Darwin, M., McElfresh, M., Shand, P. M., Xu, J., Crooker, B. C. and Spalek, J., Electronic properties of the metallic perovskite $LaNiO_3$: correlated behavior of 3d electrons. *Phys. Rev. B*, 1992, **46**(10), 6382–6386.
6. Mizusaki, J., Tabuchi, J., Matsuura, T., Yamauchi, S. and Fueki, K., Electrical conductivity and Seebeck coefficient of nonstoichiometric $La_{1-x}Sr_xCoO_{3-\delta}$. *J. Electrochem. Soc*., 1989, **136**(7), 2082–2088.
7. Zhang, W., Boyd, I. W., Elliot, M. and Herrenden-Harkerand, W., The effects of oxygen content on the magnetoresistive behaviour in La–Sr–Mn–O films grown on Si. *Appl. Phys. Lett*., 1996, **69**(25), 3929–3931.
8. Kung, P.-J., Fenner, D. B., Potrepka, D. M. and Budnik, J. I., Growth and characterization of magnetoresistive La–Ca–Mn–O films on Si (100) and Si (111) substrates. *Appl. Phys. Lett*., 1996, **69**(25), 427–429.
9. Goodenough, G. B., Electronic structure of CMR manganites. *J. Appl. Phys*., 1997, **81**(8), 5330–5335.
10. Lytle, F. W., X-ray diffractometry of low-temperature phase transformation in strontium titanate. *J. Appl. Phys*., 1964, **35**, 2212–2215.
11. Waser, R., and Smyth, D. M., Defect chemistry, conduction and breakdown mechanism of peroshite-structure titanates. In *Ferroelectric Thin Films: Synthesis and Basic Properties*, ed. J. F. Scott. Gordon and Breach, Philadelphia, 1996.
12. Vollmann, M., *Elektronische Korngrenzeigenschaften akzeptordotierter $SrTiO_3$-Dielektrika*. PhD thesis, RWTH-Aachen, VDI-Verlag, Reihe 9, Nr. 246, 1997.
13. Dietz, G. W., *$SrTiO_3$-Dünnschichten unter dem Einfluß elektrischer Gleichfelder*. PhD thesis, RWTH-Aachen, VDI-Verlag, Reihe 21, Nr. 215, 1997.
14. Hasenkox, U., Mitze, C. and Waser, R., Metal propionate synthesis of magnetoresistive La_{1-x},Ca,Sr)$_xMnO_3$ thin films. *J. Am. Ceram. Soc*., 1997, **80**(10), 2709–2713.
15. Hasenkox, U., *Nasschemische Synthese und Charakterisierung von elektronisch leitfähigen, oxidischen Dünnschichten für die Mikroelektronik*. PhD thesis, RWTH-Aachen, VDI-Verlag, Reihe 9, Nr. 306, 1999.
16. Hasenkox, U., Hoffmann, S. and Waser, R., Influence of precursor chemistry on the formation of $MTiO_3$ (M = Ba, Sr) ceramic thin films. *J. Sol-Gel Science Technol*., 1998, **12**(2), 59–72.
17. Hoffmann, S., Modifizierte Erdalkalititanat Dünnschichten für integrierte Bauelemente: *Morphologie, dielektrische Eigenschaften und Ladungstransportmechanismen*. PhD thesis, RWTH-Aachen, VDI-Verlag, Reihe 9, Nr. 288, 1998.
18. Dietz, G. W., Antpöhler, W., Klee, M. and Waser, R., Electrode Influence on the charge transport through $SrTiO_3$ thin films. *J. Appl. Phys*., 1995, **78**(10), 1–9.